

APPLICATION OF PERSISTENT SCATTERER AND SMALL-BASELINE SAR INTERFEROMETRY IN MONITORING THE SURFACE DEFORMATION IN THE CHOUHUI RIVER ALLUVIAL FAN OF CENTRAL TAIWAN

Yi-An Chen¹, Chung-Pai Chang² and Jiun-Yee Yen³

¹ PhD student, Institute of Geophysics, National Central University,
No. 300, Jhongda Rd., Jhongli, Taoyuan 32001, Taiwan; Tel: +886-3-4227151#57671;
E-mail: dgs0822.tw@msa.hinet.net

² Associate Professor, Center for Space and Remote Sensing Research, National Central University,
NO. 300, Jhongda Rd., Jhongli, Taoyuan 32001, Taiwan; Tel: +886-3-4227151#57627;
E-mail: cpchang@csrnr.ncu.edu.tw

³ Assistant Professor, Department of Natural Resource and Environmental Studies, National Dong Hwa University,
No. 1, Sec. 2, Dahsueh Rd., Shoufeng, Hualien 97401, Taiwan; Tel: +886-3-8227106#5000
E-mail: jyyen@mail.ndhu.edu.tw

KEY WORDS: Persistent Scatterer, Small-baseline, SAR Interferometry, Surface Deformation, Groundwater, Choushui River Alluvial Fan

ABSTRACT:

Groundwater overexploitation has caused serious land subsidence in the Choushui River Alluvial Fan (CRAF) area of central Taiwan. Traditionally, the extent and magnitude of the surface subsidence was determined by precise-leveling, however, the cost and spatial and temporal density of the traditional survey prevent the understanding of the full extend of the effect. In this study we implement the Persistent Scatterer and Small-baseline SAR Interferometry, which provides much better spatial resolution, to investigate the surface deformation in CRAF where the water withdraw was serious since long time.

Twenty-three radar images, acquired by the European radar satellite ENVISAT from June of 2004 to September of 2008, were used to analyze the surface deformation in the study area. From our results, the most serious subsidence areas are in the middle and distal fan of CRAF, the pass way of the Taiwan High Speed Rail, where the maximum deformation rate is nearly 7 cm/yr along the radar Line-Of-Sight direction. Moreover, it also reveals an obvious subsidence zone in the coastal industrial area of Yunlin with different deformation trend from north to south. Finally we compare our results with the precise-leveling data, the continue GPS data and groundwater level data within the region. It illustrates that the surface deformation in CRAF is related to the seasonal fluctuation of groundwater, which are the high deformation rate in dry season and the low deformation rate in wet season.

1. Introduction

Surface deformation especially caused by the groundwater overexploitation is becoming a serious problem in the world. During past decades, this problem also happens in Taiwan. Owing to the insufficiency and limitation of the surface water in the central Taiwan, groundwater resource becomes the primary water source in this area. However, when groundwater extraction exceeds the natural recharge limit continuously, severe consequences would occur, such as groundwater level dropping, sea-water intrusion, groundwater quality deterioration, land subsidence, poor drainage and flooding. (Wang et al., 1996; Hsu, 1998; Fan, 2001; Wang et al., 2003; Deng et al., 2007).

In the past few years, the region of the Choushui River Alluvial Fan (CRAF) in the central Taiwan had extensive and serious land subsidence caused by the groundwater overexploitation and slow recharge along the coastal areas (Liu and Huang, 2002; Water Resources Agency (WRA), 2001). Recently, the most notorious subsidence region gradually shifts away from the coast to the landward area of the CRAF, with a maximum subsiding rate reaching up to 6 cm/yr and an active subsiding area over 400 km² (WRA, 2010). Since 1995, the Water Resources Agency (WRA) started a long term monitoring of land subsidence in many regions of Taiwan by using precise leveling, continues Global Positioning System (GPS) and multi-level compaction wells, and provided many measures for the government to reduce subsidence, for example restriction of groundwater withdrawing, forestation, and dams constructing.

Moreover, Chen et al. (2010) demonstrated the linear relationship between surface displacement and groundwater level variation, and quantified the land subsidence phenomena by using the GPS data and groundwater level data. Hung et al. (2010) attempted to derive vertical deformation over CRAF by using differential synthetic aperture radar interferometry (DInSAR) technique, and showed the basin-like subsidence area with 10 cm/yr deformation rate in Yunlin during the period from 2006 to 2007.

Owing to the pointwise and scarce observation data acquired from leveling, GPS and compaction monitoring wells can not illustrate more detailed ground deformation in an extensive area, DInSAR technique is therefore applied to mitigate the uncertainty of the low observation density and to provide 2-D information of deformation. Besides, the

agriculture region like CRAF is covered with many fishponds. And thus, it leads surface property variation with different seasons and the atmosphere-induced error is caused the spatial decorrelation and degraded the accuracy of measurement respectively (Hung et al., 2010). In order to overcome these deficiencies, we utilize the persistent scatterer and small-baseline SAR interferometry to extract the surface deformation in CRAF, and compare the InSAR result with leveling, GPS and groundwater level data to discuss the relationship between the ground deformation and groundwater level variation. From our result, the surface deformation in CRAF is related to the seasonal fluctuation of groundwater, which shows a high deformation rate in dry season and a low deformation rate in wet season.

2. Background

The Choshui River Alluvial Fan, the most important agriculture area in Taiwan, comprises Changhua and Yunlin counties, and it is bordered by the Wu river to the north, the Beigang river to the south, the western part of Bagua-Douliu hills to the east and the Taiwan strait to the west, respectively (Fig.1(a)). The total area of the alluvial fan is nearly 1800 km² and with a general elevation between 0 and 100 m above sea level (Central Geological Survey (CGS), 1999; Liu et al., 2004).

As result of the complex characteristics of the formations in the CRAF, formed by frequent flooding and channel migration of the Choshui river, this area can be divided into three geological section from east to west which are the proximal fan, the middle fan and the distal fan, respectively (CGS, 1999). Drilling logs data of the CRAF present the consists of several unconfined and confined aquifers of Holocene sediments, which contain interbedded or lens-structured clay, fine sand, medium fine sand, coarse sand, and gravel layers and are separated by impermeable marine mud layers (Water Conservancy Agency (WCA), 1997; Chen and Yuan, 1999). The thickness of the sediments is 750 to 3,000 meter, and the mean grain size is decreasing from proximal fan to distal fan. Based on the sedimentological data, rock properties, fossils and permeability, the hydrogeology model of the CRAF can be considered forming an inter-layering of four aquifers and four aquitards (Fig.1(b)). Moreover, these four aquifers in the proximal fan are essentially connected, and the second aquifer with the largest extension in the CRAF is the major aquifer for withdrawing because of the acceptable depth and the thickest thickness of all aquifers (CGS, 1999; Liu et al., 2001). According to previous researches, the CRAF area has more than 110,000 wells near the middle and the distal fan (WRA, 2010). The geological characteristics of the middle and the distal fan mainly consist of fine sand, medium fine sand and clay which are able to be easily compressed. Thus, the groundwater overexploitation is result in groundwater level dropping and even causes severer land subsidence problem.

In recent years, the remote sensing techniques have gradually been applied to geodetic and geological surveys, and have become crucial monitoring techniques for surface deformation. Chen et al. (2010) utilize the GPS and groundwater level data to prove a negative and linear relationship between the changes of elevation and overdraft of groundwater in the CRAF. For the most parts, the major mechanism for the land subsidence is affected by the current groundwater level fluctuation and a long term trend caused by excessive extraction during previous times in aquifers. The DInSAR result from Hung et al. (2010) shows many minor and locally distributed displacements in Yunlin which are not detected by leveling. Moreover, the subsidence area in Yunlin is basin-like and the largest relative displacement rate is nearly 10 cm/yr in Yuanchang Township during 2006 to 2007. The RMS between DInSAR and leveling reaches 1-2 cm/yr from the comparison of vertical deformation between DInSAR and leveling.

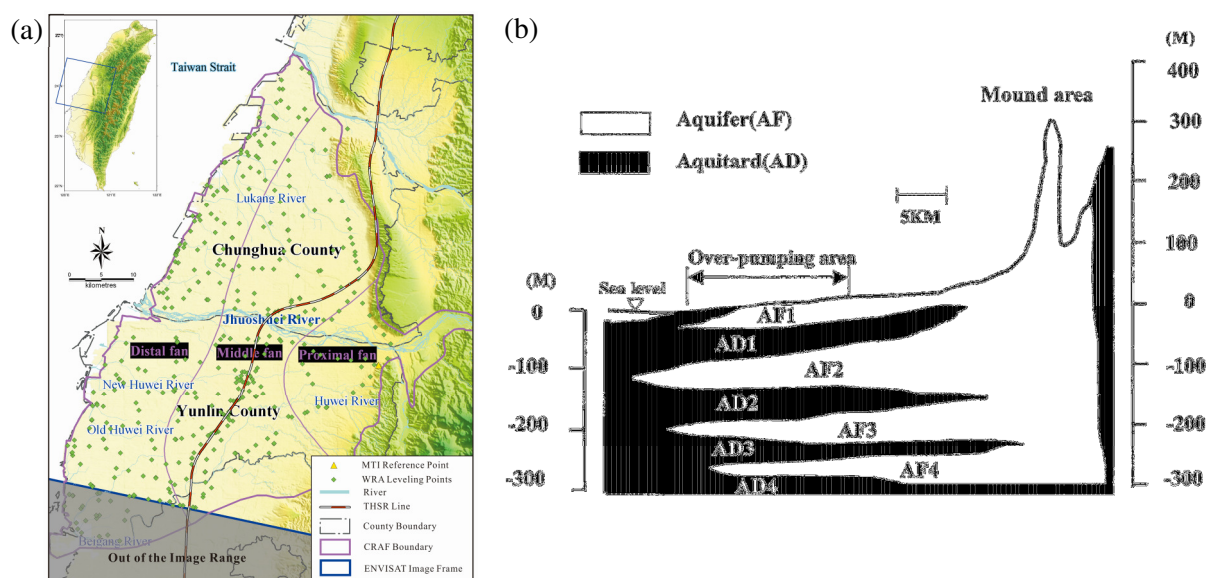


Figure.1 (a) The geographical location of the Choshui River Alluvial Fan and the distributions of leveling benchmarks (green points) and the names of counties in the CRAF are shown here. The yellow triangle “WR12” represents the control benchmark for leveling and MTI (reference point). (b) The conceptual hydrogeology model profile of the CRAF (Liu et al., 2004). Based on the sedimentological data, rock properties, fossils and permeability,

this model can be considered to form an inter-layering of four aquifers and four aquitards. The four aquifers in the proximal fan are essentially connected.

3. Methods and Data Used

In the past decades, synthetic aperture radar interferometry has been proved to be a powerful and effective geodetic technique, with high spatial resolution, sub-centimeter accuracy and useful observation cadence (~ 1 pass month⁻¹), for measuring surface deformation, neotectonic activities and natural hazards (e.g. Chang et al., 2010; Yen et al., 2011). Nevertheless, due to the CRAF surrounds a wide range of agriculture area and many fishponds, the different surface features with time and the variation of water vapor stratification between satellite passes would easily cause spatial decorrelation in conventional InSAR, and lead to a degraded accuracy in the deformation measurements. Thus, with the intention of overcoming the limitation on InSAR technology, we applied time series InSAR techniques for the surface deformation observing over the CRAF.

3.1 Methods

Recently there are two different categories of the time series InSAR technique, persistent scatterer (PS) methods (e.g. Ferretti et al. 2001; Hooper et al. 2004; Kampes 2005; van der Kooil et al., 2006) and small baseline (SB) methods (e.g. Berardino et al. 2002; Schmidt and Bürgmann 2003). A new algorithm developed by Hooper (2008) is to combine the advantages of these two approaches. Maximizing the spatial coverage of useful signal and allowing more reliable estimation of integer phase-cycle ambiguities presenting in the data are the most important improvements in the new algorithm. Later the multi-temporal InSAR method is success to apply for several studies (Sturkell et al., 2009; Yen et al., 2011). The PS algorithm and the SB algorithm that we use are clearly described in Hooper et al. (2007, 2008), involving with estimating phase contributions from various terms, where the phase from the x -th pixel in the i -th interferogram (ϕ_{int}) is:

$$\phi_{int,x,i} = \phi_{def,x,i} + \phi_{orb,x,i} + \phi_{\epsilon,x,i} + \phi_{atm,x,i} + \phi_{n,x,i} \quad (1)$$

where ϕ_{def} , ϕ_{orb} , ϕ_{ϵ} , ϕ_{atm} and ϕ_n present the phase variation due to the movement of the pixel in the satellite line-of-sight (LOS) direction, the satellite orbit inaccuracies, the digital elevation model (DEM) error (look angle error), the atmospheric disturbance along the radar wave paths and the general noise term (e.g. thermal noise, coregistration errors and uncertainty of the phase position), respectively. Several error sources which are in the observation itself or due to the processing affect the InSAR data. In the equation (1), to minimize the last four terms is required, because these four terms confound the deformation signal that we are interested in. Owing to the deformation, atmosphere and orbit error terms are correlated spatially, and the DEM error term tends to be partly spatially correlated, the mathematical algorithm can be designed to estimate these terms. Moreover, the selected PS pixels are those which ϕ_n are too small enough to obscure the deformation signal completely. Hence, the phase caused by surface deformation can be obtained by subtracting the estimated error terms from the initial phase of the interferogram. Nevertheless, result in maximizing the correlation between the SAR images, the conditions of perpendicular, temporal and Doppler baselines are all considered (Fig.2).

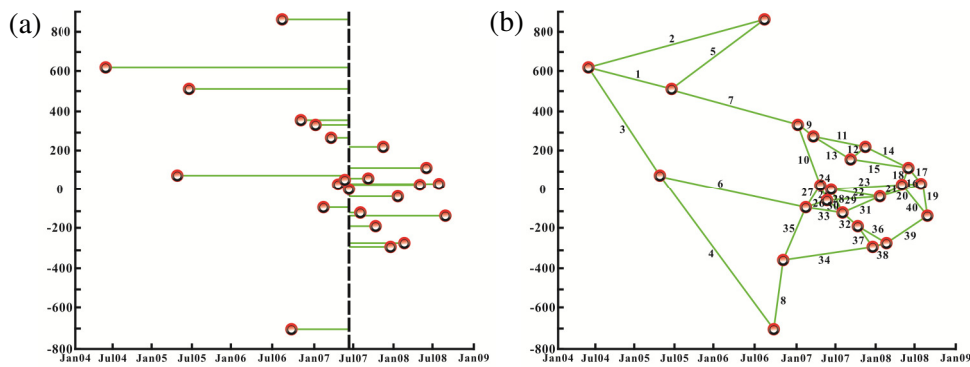


Figure.2 (a) Radar images and baseline spatial information used in the PS processing. (b) Radar images and baseline spatial information used in the SB processing. Vertical axes are perpendicular baselines of images, and horizontal axes are acquisition dates of radar images. Red circles and green lines represent the radar images and the formed interferograms, respectively.

3.2 Data Used

In this study, all used images are acquired from European Space Agency ENVISAT satellites, which are belong to the scene of descending track 461/ frame 3123 from June of 2004 to September of 2008 (Tab.1). The ASAR sensor onboard the ENVISAT satellite operates in C-band with a wavelength of 56.2 mm and the size of the image frame is nearly 100 km x 100 km. The Interferometric processing was performed using the Doris software developed by the

Delft Institute for Earth-Oriented Space Research (DEOS), and the multi-temporal InSAR processing and the 3-dimensional spatio-temporal unwrapping was done by applying StaMPS/MTI software developed by Hooper et al.(2007, 2008). The SRTM digital elevation model that we used sampled into a 25 m pixel spacing grid to estimate and to remove the topographic contribution. The ENVISAT precise orbits released by DEOS are used to avoid and correct most errors caused by the orbits. The precise leveling, GPS and groundwater level data provided from the Water Resources Agency, are used to calibrate the InSAR result and to discuss the relationship of surface deformation and groundwater level fluctuation.

Table.1 Parameters of the ENVISAT images that we used in this paper. The master image is fixed on 6 November, 2004. Information of all the images, including date of acquisition, perpendicular baseline, and the interval time with the master image are shown. Track = 232, Frame = 3123. (^a length of perpendicular baseline component; ^b the interval time with the master image)

Image No.	Year/Month/Day	Baseline ^a (m)	Time ^b (days)	Category of Image	Image No.	Year/Month/Day	Baseline ^a (m)	Time ^b (days)	Category of Image
1	2004/06/03	634.7	1120	Slave	13	2007/08/02	-108.6	35	Slave
2	2005/05/19	83.1	770	Slave	14	2007/09/06	159.1	70	Slave
3	2005/06/23	518.4	735	Slave	15	2007/10/11	-190.9	105	Slave
4	2006/08/17	868.7	315	Slave	16	2007/11/15	219	140	Slave
5	2006/09/21	-701.2	280	Slave	17	2007/12/20	-285.3	175	Slave
6	2006/10/26	355	245	Slave	18	2008/01/24	-37.5	210	Slave
7	2007/01/04	332.8	175	Slave	19	2008/02/28	-264.3	245	Slave
8	2007/02/08	-79.4	140	Slave	20	2008/05/08	28.5	315	Slave
9	2007/03/15	270.5	105	Slave	21	2008/06/12	121.5	350	Slave
10	2007/04/19	26.4	70	Slave	22	2008/08/21	34.1	420	Slave
11	2007/05/24	-50.7	35	Slave	23	2008/09/25	-126.6	455	Slave
12	2007/06/28	0	0	Master					

4. Results

4.1 Interferometry Result

In this study, 23 ENVISAT radar images, ranged from June 2004 to September 2008, are applied to form 22 PS interferograms and 40 SB interferograms. Within the 1800 km² of our study area, more than 400,000 stable targets are available in the ENVISAT dataset, and the spatial observation density is about 230 points km⁻². In figure 3(a), the warm colors and the cold colors represent the shortening and elongation along the radar LOS direction relative to the master image, respectively. Therefore, the unwrapped results of time series deformation map (Fig.3(b)) illustrate that the continual deformation areas are mainly in the middle and distal fan of the CRAF.

Due to only the relative slant range displacement along the satellite view angle in the radar interferometric result, we used the benchmark “WR12”, installed by the WRA and is considered stable to be the control benchmark for precise leveling in the CRAF, as the reference point to adjust our MTI result. After this adjustment, the slant range deformation pattern shown in Fig. 6 can be considered as the near-true surface deformation. The most conspicuous deformation pattern is the subsidence inside the CRAF (the middle and distal fan), with the maximum relative deformation rate nearly 7 cm/yr along the radar LOS direction. Still, it reveals an obvious subsidence zone in the coastal industrial area of Yunlin with a different deformation trend from north to south (red rectangle in Fig.3(a))

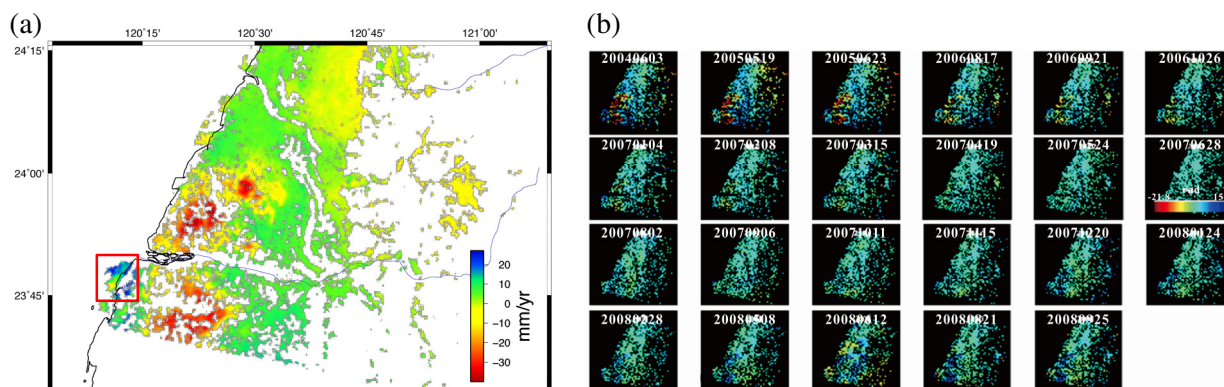


Figure.3 (a) LOS displacement rates from MTI over 2004 to 2008. The red rectangle shows an obvious subsidence zone in the coastal industrial area with no leveling points. (b) LOS displacements from 22 slave images relative to the epoch of the master image (June 28, 2007).

4.2 Data Comparisons

Note that radar interferometric result illustrates the relative displacement; hence, it needs to be compared to other geodetic data, e.g. the precise leveling and GPS data, to obtain more complete understanding of the regional deformation. The results of vertical displacement rate are obtained by annual leveling survey from 2004 to 2008 in the CRAF, as well as the continue GPS data (SSES Station where is in the distal fan) between the same period are provided from the WRA. In order to avoid missing data, MTI data is interpolated previously using nearest-neighbor processing and the interpolation is limited to existing persistent scatterers within 1 km. Therefore, the MTI information is extracted in the same locations of all benchmarks within a 500-meter radius in the CRAF. The comparison between our MTI results and leveling data (524 benchmarks) presents the relationship between both geodetic techniques is linear (the correlation coefficient is about 0.9, the slope is 0.74 and the intercept is 0.49), and the slope reveals the underestimate in MTI results (Fig.4(a)). Figure.4(b) shows the distribution of the benchmarks and the distribution of the differences. Moreover, comparing our MTI time series deformation results with the continues GPS data in the same location illustrates that the variation of ground elevation was gradually declining with time, as well as the deformation trends of two measurements are extremely similar (Fig.5(a)). Meanwhile, the subsidence trend was alleviating in the wet season (from April to September), but aggravating dramatically in the dry season (from October to March) during 2004 to 2008. Ground elevation changing is usually affected by many factors, such as groundwater level fluctuation and tectonic activities etc. For the most part, the major mechanism for the subsidence in the CRAF is not only the dramatic fluctuation of groundwater level but also the overexploitation of groundwater resource (Chen et al., 2010). In figure 5(b), it illustrates the relationship between MTI and groundwater level data (Hefeng groundwater site with the 3rd and the 4th aquifers in the distal fan). The surface deformation is consequent to the groundwater level descending (the time delay phenomena), as well as the deformation pattern is highly related with the groundwater fluctuations in the underlying two aquifers.

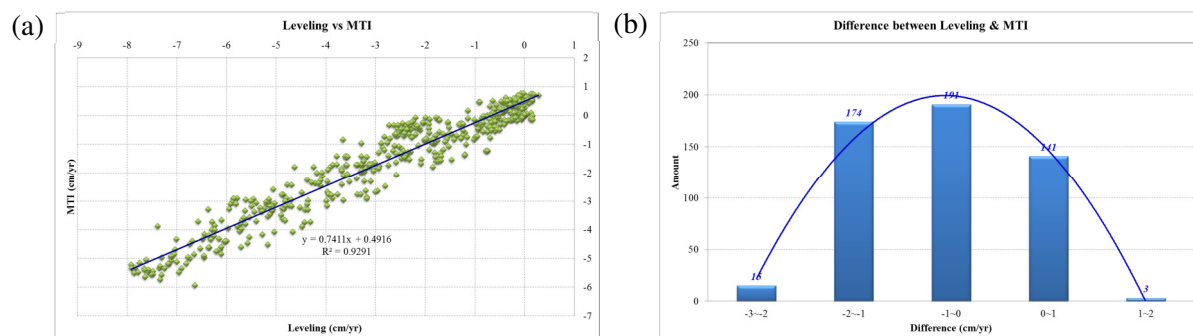


Figure.4 The comparison of MTI and Leveling data. (a) The distribution of the comparison between both geodetic techniques. (b) The distribution of the differences between MTI and leveling data. The RMS value of the differences is about 1 cm/yr. Of the 524 differences, 332 values (absolute) are less than 1 cm/yr, other values are between 1 and 3 cm/yr. This suggests that 63.4% of the MTI-derived rates reach an accuracy of 1 cm/yr at least.

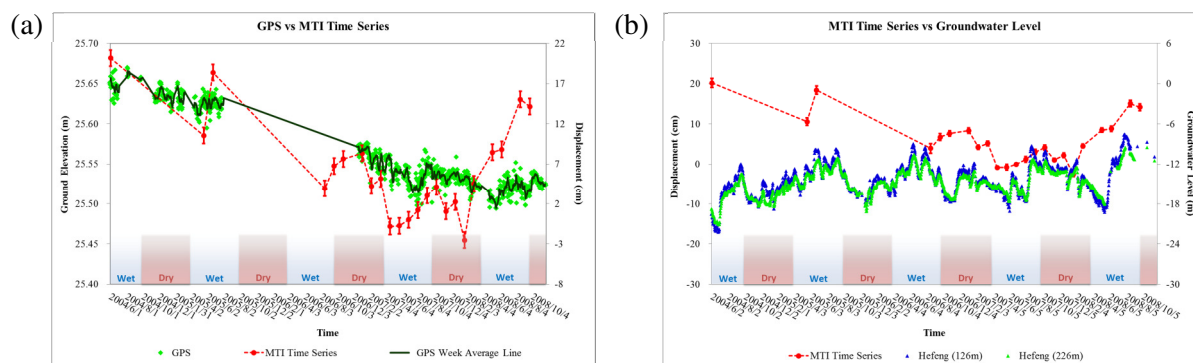


Figure.5 (a) Daily GPS data compare with MTI data. The deformation trend of MTI data is similar to GPS data, and the variation is more serious in dry seasons than in wet seasons. (b) The comparison of MTI and daily groundwater level data. The deformation pattern is highly related with the groundwater fluctuations in the underlying two aquifers.

5. Discussion

From the monitoring results in the CRAF area, PSI results are not only high in spatial resolution but also good in measuring accuracy. Nevertheless, it could present the information about surface deformation even in some small areas where no leveling points or GPS stations. Moreover, the results from interferometry could be compared with other geodetic data to calibrate or with geological data to understand more comprehensive deformation factors. Analysis of these three observations, e.g. leveling, GPS and MTI, indicate that calibrated interferometry results are highly correlated to GPS deformation rate and the similar deformation trend in time series. However, there are still

some differences between these measurements which might be attributed to several factors, such as look angle correction factor, line-of-sight measurement ambiguity, differences in observation duration and spatial interpolation of the MTI results.

On the other hand, in comparison result between MTI and groundwater level data, it reveals the relative displacement was uplifting in the wet season but subsiding in the dry season during 2004 to 2008. Owing to the insufficient of groundwater level data (only one site), the relationship between geological characterizes, groundwater level variation and ground deformation is needed to study more comprehensively in the further. Moreover, our result of this study might provide not only useful information to understand the wide range deformation, but also a reference for land and water resources management in serious subsidence areas.

Reference

- Berardino, P., Fornaro, G., Lanari, R., and Sansosti, E., 2002. A new algorithm for surface deformation monitoring based on small baseline differential SAR interferograms. *IEEE Transactions on Geoscience and Remote Sensing*, 40, 2375-2383.
- Central Geological Survey (CGS), 1999. The investigation of hydrogeology in the Choshui River alluvial fan, Taiwan. Central Geological Survey of Taiwan, Taipei.
- Chang, C.P., Yen, J.Y., Hooper, A., Chou, F.M., Chen, Y.A., Hou, C.S., Hung, W.C. and Lin, M.S., 2010. Space-borne Radar for surface deformation analysis of northern Taiwan area, Differential and Persistent Scatterer Interferometry. *Terr. Atmos. Ocean. Sci.*, 21, 447-461.
- Chen, C.H., Wang, C.H., Hsu, Y.J., Yu, S.B., Kuo, L.C., 2010. Correlation between groundwater level and altitude variations in land subsidence area of the Choshuichi Alluvial Fan, Taiwan. *Engineering Geology*, 115, 122-131
- Chen, W.F., and Yuan, P., 1999. A preliminary study on sedimentary environments of Choshui fan-delta. *J. Geol. Soc. China* 42, 269-288.
- Deng, Q.H., Ma, F.S., Yuan, R.M., and Yao, B.K., 2007. Geological environment problems caused by controlling groundwater exploitation in Jiangyin city. *Journal of China University of Mining & Technology*, 17, 85-89.
- Ferretti, A., C. Prati, C., and Rocca, F., 2001. Permanent scatterers in SAR interferometry. *IEEE Trans. Geosci. and Remote Sens.*, 39(1), 8-20.
- Hooper, A., Zebker, H., Segall, P., and Kampes, B., 2004. A new method for measuring deformation on volcanoes and other natural terrains using InSAR persistent scatterers. *Geophysical Research Letters* 31, L23611.
- Hooper, A., Segall, P., and Zebker, H., 2007. Persistent scatterer InSAR for crustal deformation analysis, with application to Volcán Alcedo, Galápagos. *Journal of Geophysical Research*, 112, B07407.
- Hooper, A., 2008. A multi-temporal InSAR method incorporating both persistent scatterer and small baseline approaches. *Geophys. Res. Letters*, 35, L16302, doi:10.1029/2008GL034654.
- Hsu, S.K., 1998. Plan for a groundwater monitoring network in Taiwan. *Hydrogeol. J.*, 6, 406-415.
- Hung, W.C., Hwang, C.W., Chang, C.P., Yen, J.Y., Liu, C.H., and Yang, W.H., 2010. Monitoring severe subsidence in Taiwan by multi-sensors: Yunlin, the southern Choshui River Alluvial Fan. *Environmental Geology*, 59(7), pp. 1535-1548.
- Kampes, B.M., 2005. Displacement Parameter Estimation Using Permanent Scatterer Interferometry. PhD thesis, Delft University of Technology.
- Liu, C.H., and Huang, C.T., 2002. Taiwan land subsidence caused by groundwater overdrafting. *J. Civ. Hydraul. Eng.*, 29, 47-57.
- Liu, C.H., Pan, Y.W., Liao, J.J., Huang, C.T., and Ouyang, S., 2004. Characterization of land subsidence in the Choshui River alluvial fan, Taiwan. *Environmental Geology*, 45, 1154-1166.
- Liu, C.W., Lin W.S., Shang, C., and Liu, S.H., 2001. The effect of clay dehydration on land subsidence in the Yun-Lin coastal area, Taiwan. *Environ Geol*, 40(4/5), 518-527
- Fan, K.L., 2001. Some coastal environmental problems in Taiwan. *Acta Oceanogr. Taiwan*, 39, 1-10.
- Schmidt, D.A. and Bürgmann, R., 2003. Time-dependent land uplift and subsidence in the Santa Clara valley, California, from a large interferometric synthetic aperture radar data set. *Journal of Geophysical Research*, 108, 2416-2428.
- Sturkell, E., Einarsson, P., Sigurdsson, F., Hooper, A., Ofeigsson, B.G., Geirsson, H., and Olafsson, H., 2009. Katla and Eyjafjallajökull volcanoes. *Developments in Quaternary Science*, 13, pp.5-21.
- van der Kooij, M., Hughes, W., Sato, S., and Poncos, V., 2006. Coherent target monitoring at high spatial density: Examples of validation results, *Eur. Space Agency Spec. Publ.*, SP-610.
- Wang, C.H., Peng, T.R., and Liu, T.K., 1996. The salinization of groundwater in the northern Lan-Yang Plain, Taiwan: stable isotope evidence. *J. Geol. Soc. China*, 39, 627-636.
- Wang, C.H., Kuo, C.H., Peng, T.R., Chen, W.F., Liu, T.K., and Chiang, C.J., 2003. Isotope characteristics of groundwaters in the Pingtung Plain, southern Taiwan. *W. Pac. Earth Sci.*, 3, 1-8.
- Water Conservancy Agency (WCA), 1997. Preliminary Analyses of Groundwater Hydrology in the Choshui Alluvial Fan. Groundwater Monitoring Network Program Phase I, Ministry of Economic Affairs, Taiwan.
- Water Resources Agency (WRA), 2001. Report of the Monitoring, Investigating and Analyzing of Land Subsidence in Taiwan (1/4). Ministry of Economic Affairs, Executive Yuan, Taipei, Taiwan.
- Water Resources Agency (WRA), 2010. Analyzing, Monitoring and Investigating Land Subsidence in Changhwa, Yunlin, Chiayi and Tainan area in 2010. Ministry of Economic Affairs, Executive Yuan, Taipei, Taiwan.
- Yen, J.Y., Lu, C.H., Chang, C.P., Hooper, A., Chang, Y.H., Liang, W.T., Chang, T.Y., Lin, M.S. and Chen, K.S., 2011. Investigating active deformation in the northern Longitudinal Valley and City of Hualien in eastern Taiwan using Persistent Scatterer and Small-Baseline SAR Interferometry. *Terr. Atmos. Ocean. Sci.*, 22(3), doi: 10.3319/TAO.2010.10.25.01(TT)